Self-organized Multi-robot Task Allocation using Attractive Field Model: Comparison of Centralized and Local Communication

Md Omar Faruque Sarker and Torbjørn S. Dahl

***Abstract*—This paper proposes to solve multi-robot task-allocation (MRTA) problem using a set of previously published generic rules for self-organised division of labour derived from the observation of ant, human and robotic social systems. The concrete form of these rules, the *attractive filed model* (AFM), provide sufficient abstraction to accommodate different sensing and communication models. We have validated the effectiveness of AFM for MRTA using two bio-inspired communication and sensing strategies: *global sensing - no communication* and *local sensing - local communication*. The former is realized using a centralized communication system and the latter is emulated as a peer-to-peer local communication scheme. Both strategies have been evaluated using 16 e-puck robots.**

I. Introduction

MULTI-ROBOT systems can provide high levels of performance, fault-tolerance and robustness in complex and distributed tasks through parallelism and redundancy [1]. *But how those tasks can be allocated dynamically among multiple robots?* Traditionally, this issue has been identified as *multi-robot task allocation* (MRTA) [2], analogous to *division of labour* (DOL) in biological and human social systems [3]. MRTA is generally defined as the problem of assigning tasks in an appropriate time to the appropriate robots considering the changes in task-requirements, team-performance and the environment [4]. The complexities of the *distributed* MRTA problem arise from the fact that there is no central planner or coordinator for task assignments, and in a large multi-robot system, robots generally have limited abilities to sense, to communicate and to interact locally.

M. O. F. Sarker and T. S. Dahl is with Cognitive Robotics Research Centre, University of Wales, Newport, Newport Business School, Allt-yr-yn Campus Newport, NP20 5DA, United Kingdom. e-mail: Mdomarfaruque.Sarker@newport.ac.uk

Within the context of the Engineering and Physical Sciences Research Council (UK) project, "Defying the Rules: How Self-regulatory Systems Work", we have developed the *attractive field model* (AFM) [5], a model of self-regulated DOL formed by the studies of self-regulated task-allocation in ant, human and robotic social systems. AFM suggests four generic rules to explain self-regulation in those social systems. These four rules are: *continuous flow of information*, *concurrency*, *learning* and *forgetting*. Primarily, these rules help to derive local control laws for regulating an individual's task-allocation behaviour in such a way that facilitates DOL in an entire group.

In biological social systems, communications among the group members, as well as the perception of tasks, are two key components of self-organized DOL. In robotics, existing self-organized task-allocation methods rely heavily upon local sensing and local communication between individuals. AFM however, differs significantly in this point. Being a highly abstract model, it avoids a strong dependence on any specific communication strategy. AFM uses the abstraction of attractive fields or continuous flows of information from tasks to agents. In order to enable continuous flow of information in our multi-robot system, we have implemented two types of sensing and communication strategies inspired by the self-regulated DOL found in two types of social wasps: *polistes* and *polybia* [6]. In polistes wasps reproductive females establish colonies alone or in small groups (in the order

of 10^2), but independent of any sterile workers. But in polybia wasps, a swarm of workers and queens initiate colonies consisting of several hundreds to millions of individuals. Polistes wasps do not rely on any cooperative task performance while swarm founders interact with each-other locally to accomplish their tasks. The work mode of polistes wasps can be considered as *global sensing - no communication (GSNC)* in which the individuals sense the task requirements throughout a small colony and do these tasks without communicating with each other. The work mode of the polybia wasps, on the other hand, can be treated as *local sensing - local communication (LSLC)* in which the individuals can only sense tasks locally due to the large colony size and can communicate locally to exchange information. This study emulates these two types of wasps behaviours in a multi-robot manufacturing shop-floor scenario using AFM.

The main contributions of this paper are as follows. This study compares the performance of two bio-inspired sensing and communication strategies in producing self-regulated MRTA. Besides, this study presents a novel taxonomy of MRTA solutions derived based on the organization of task-allocation, interaction and communication among robots.

This paper has been organized as follows. Section 2 reviews the related literature on MRTA. Section 3 presents the new taxonomy of MRTA solutions. Section 4 presents AFM based task-allocation solution for multi-robot systems. Section 5 describes our centralized and local communication schemes used in this study. Section 6 and Section 7 present the design and implementation of our experiments respectively. Section 8 describes our results. Section 9 discusses the performance of self-regulated MRTA under both centralized and local communication strategies. Section 10 concludes this paper and suggests some directions for future works.

II. Related work

Since the 90s, many robot control architectures have been designed and evolved to address various MRTA issues from different perspectives. Based on the high-level design of those solutions, we have classified them into two broad categories: i) explicit task-allocation and ii) bio-inspired self-organized task-allocation. Early research on explicit task-allocation was dominated by explicit cooperation [7], use of dynamic role assignment [8] and market-based bidding approach [9]. These approaches are intuitive and comparatively straight forward to design and implement and can be analysed formally. However, these approaches typically work well only when the number of robots are small (≤ 10) [10].

Task performance in self-organized approaches, on the other hand, relies on the collective behaviours resulting from the local interactions of many simple and mostly homogeneous or interchangeable agents. Robots choose their tasks independently using general principles of self-organization [11]. Moreover interaction among individuals and their environment can be modulated by stigmergic, local and global communications. Among many variants of self-organized task-allocation mechanisms, the most common type is response threshold-based task-allocation [12]. In this approach, a robot's decision to select a particular task depends largely on its perception of a stimulus, e.g., the demand for a task to be performed, and its corresponding response threshold for that task.

Under the deterministic response-threshold approach, each robot has an activation threshold for each task that needs to be performed. When a particular task-stimulus exceeds a predefined threshold the robot starts working on that task, typically reducing their related stimuli. When the task-stimuli falls below the fixed threshold the robot abandons that task. This type of approach has been effectively applied in foraging [13], [14] and aggregation [15]. The fixed response threshold can initially be same for all robots [16] or they can be different according robot capabilities or the configuration of the system [14]. Adaptive response-threshold models change the thresholds over time. A robot's response threshold for a given task is often decreased as a result of the robot performing that task. This enables a robot to select that particular task more frequently or in other words specialise on that task [12], [15]. Unlike the deterministic approach, probabilistic approaches

offer a selection process based-on a probability distribution over the tasks. In this case, all tasks commonly have at least a small, non-zero probability of being chosen. Bio-inspired, self-organized MRTA mechanisms rely on a much smaller degree of modelling the environment, tasks or robot capabilities. Most existing research in this area considers a single global task e.g. foraging, area cleaning and box-pushing focusing on the design of individual robot controllers that can accomplish that task [4].

In an arbitrary event handling domain, it is found that explicit task-allocation was more efficient when the required information could be captured accurately [17]. The threshold-based approach offered similar quality of allocation at a fraction of cost in noisy environment. Gerkey and Mataric [4] compared the complexity and performance of key explicit task-allocation architectures, including ALLIANCE [7], the Broadcast of Local Eligibility [18], M+ [19], MURDOCH [20], First piece auctions [9] and Dynamic role assignment [8]. The computational and communication requirements of those systems were expressed as a function of the number of robots and tasks. Although the study does not explicitly measure the scalability of the architectures, it clearly shows that many explicit task-allocation mechanisms will fail to scale well in environments where the number of robots and tasks are large and the communication bandwidth and processing power of individual robots are limited.

III. A TAXONOMY OF MRTA

In order to understand the interplay among task-allocation, communication and interaction of a particular MRTA approach we have presented these aspects in two 2D characteristic plots.

Fig. 1 presents the classification of MRTA solutions based on task-allocation and communication strategies used to disseminate information. Here horizontal axis shows the number of active nodes that provides the task-allocation to the group. The origin of this axis represents the explicit task-allocation by a single centralized entity. For example, in any explicit task-allocation approach, we can use one of the robots (aka *leader*) to manage the task-allocation process. In many explicit task-allocation methods, e.g. in market-based systems, multiple nodes can act as mediators (task-allocators), or for a small number of robots, each robot acts as an independent task-allocator e.g. as found in ALLIANCE architecture.

The right extreme of horizontal axis in Fig. 1 represents the swarm task-allocation method usually employed for large number of robots. This method is fully distributed, i.e. each robot selects its tasks independently and without the help of a leader. However, robots might be dependent on other entities for getting the latest *information* about tasks. In a recent study on swarm-robotic flocking, it was shown that a swarm can be guided to a target by a few informed individuals or leaders while the remaining robots remain self-organized [21]. Task-allocation in a swarm of robots through one central entity may be rare since one of the major motivations behind swarm robotic systems is to make the swarm task-allocation more robust by avoiding single point of failure.

The vertical axis in Fig. 1 shows the communication range of individual entities. In case of implicit communication via stigmergy in swarm task-allocation this range has been considered as zero. On the other hand, in case of explicit task-allocation a global range can cover all entities. In this research we have placed our two kinds of communication strategies vertically aligned with swarm task-allocation. *AFM centralized communication* represents a GSNC based system where communication range is global and task-allocation is fully distributed. Similarly, AFM local communication also represents the the fully distributed task-allocation but with limited communication range under LSLC strategy.

The information flow caused by different levels of communication and interaction among multiple robots has been depicted in Fig. 2. Two extreme forms of information flow is shown here. *Insufficient information flow* occurs when individual's communication range is low and their interaction is limited. In such cases, system designer can find suitable trade-off to get a balanced information flow by increasing communication range or interaction frequency or both. On another extreme of this

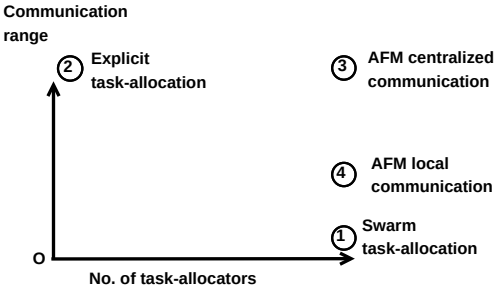

Fig. 1: Classification of MRTA solutions based on task-allocation and communication strategies

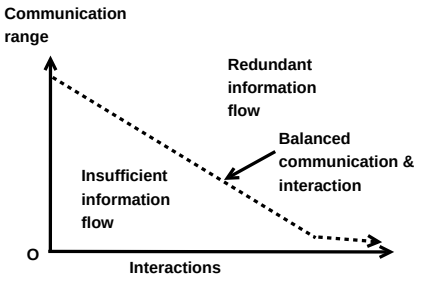

Fig. 2: Information flow caused by different levels of communication and interaction

situation, we can find lots of *redundant information flow* where all individuals are both communicating and interacting. Thus the dotted line in the plot refers to a balanced communication and interaction. This dotted line does not completely intersect the horizontal line since when the communication range is limited to the next neighbour, individuals can still continue to interact with others as much as possible.

The presence of interaction can be due to the nature of the problem, e.g. cooperation is necessary in co-operative transport tasks. Alternately, this interaction can be a design choice where interaction can improves the performance of the team, e.g. cooperation in cleaning a work-site is not necessary but it can help to improve the efficiency of this task. Various task-allocation methods rely upon variable degrees of robot-robot communications. The communication capabilities of individual robots can limit (or expand) the level of interaction that can be made in a given group. Thus considering the interaction requirements of a MRTA problem, the system designer can select suitable communication strategies that both minimizes the communication overhead and maximizes the performance of the group. Alternately, the communication capabilities of the robots can guide a system designer to design interaction rules of a robot team, e.g. the specification of a robot's on-board camera can dictate the degree of possible visual interactions among robots. The suitable trade-off between these options can give a balanced design for a better MRTA solution.

IV. Task-allocation using AFM

AFM provides an abstract framework for solving task-allocation problem among multiple agents. The mathematical model has been discussed in [5] and an experimental validation of AFM in multi-robot system has been reported in [22]. Here we have briefly summarized the core concepts of AFM within the context of a manufacturing shop-floor scenario.

AFM formalises the four requirements of self-organised social systems (Section 1) in terms of the relationships between properties of individual agents and of the task-allocation system as a whole. Here, tasks can be described as the sources of the attractive fields with varying levels of urgencies. They encode the strength of the attractive fields as perceived by the agents. All communication is considered part of the attractive fields. There is also a permanent field representing the *no-task* option of not working in any of the available tasks. This option is modelled as a random walk. The edges of the AFM network between tasks and agents are weighted and the value of this weight describes the strength of the stimulus as perceived by the agents. In a spatial representation of the model, the strength of the field depends on the physical distance of the agent to the source. The strength of a field is increased through the sensitisation of the agent through experience with performing the task.

Under our manufacturing shop-floor scenario, each task represents a manufacturing machine that is capable of producing goods from raw materials, but they also require constant maintenance works for stable operations. Let W_j be a finite number of material parts that is loaded into a machine j in the beginning of its production process and in each time-step, ω_j units of material parts can be processed ($\omega_j \ll W_j$). So let Ω_j^p be the initial production workload of j which is simply: W_j/ω_j unit. We assume that all machines are identical. In each time step, each machine always requires a minimum threshold number of robots *(μ)* to meet its constant maintenance work-load, Ω_j^m unit. However, if μ or more robots are present in a machine for production purpose, we assume that, no extra robot is required to do its maintenance work separately.

Now let us fit the above production and maintenance work-loads and task performance of robots into a unit task-urgency scale. Let us divide our manufacturing operation into two subsequent stages: i) *production cycle* (production and maintenance tasks), and ii) *maintenance cycle* (maintenance tasks only). Initially a machine starts working in production cycle. When there is no production work left, then it enters into maintenance cycle. Under both modes, let α_j be the amount of workload occurs in a unit time-step if no robot serves a task and it corresponds to a fixed task-urgency $\Delta\phi_{INC}$. On the other hand, let us assume that in each time-step, a robot, i, can decrease a constant workload β_i by doing some maintenance work along with doing any available production work. This corresponds to a negative task urgency: $-\Delta\phi_{DEC}$. So, at the beginning of production process, task-urgency, occurred in a machine due to its production work-loads, can be encoded by Eq. 1.

$$\Phi_{j,INIT}^P = \Omega_j^p \times \Delta\phi_{INC} + \phi_j^{m0} \tag{1}$$

where ϕ_j^{m0} represents the task-urgency due to any initial maintenance work-load of j. Now if no robot attends to serve a machine, each time-step a constant maintenance workload of α_j^m will be added to j and that will increase its task-urgency by $\Delta\phi_{INC}$. So, if k time steps passes without any production work being done, task urgency at k^{th} time-step will follow Eq. 2.

$$\Phi_{j,k}^P = \Phi_{j,INIT}^P + k \times \Delta\phi_{INC} \tag{2}$$

However, if a robot attends to a machine and does some production works from it, there would be no extra maintenance work as we have assumed that μ = 1. Rather, the task-urgency on this machine will decrease by $\Delta\phi_{DEC}$ amount. If ν_k robots work on a machine simultaneously at time-step k, this decrease will be: $\nu_k \times \Delta\phi_{DEC}$. So in such cases, task-urgency in $(k+1)^{th}$ time-step can be represented by:

$$\Phi_{j,k+1}^P = \Phi_{j,k}^P - \nu_k \times \Delta\phi_{DEC} \tag{3}$$

At a particular machine j, once $\Phi_{j,k}^P$ reaches to zero, we can say that there is no more production work left and this time-step k can give us the *production completion time* of j, T_j^P. Average production time-steps of a shop-floor with J machines can be calculated by the following simple equation.

$$T_{avg}^P = \frac{1}{J}\sum_{j=1}^{M} T_j^P \tag{4}$$

T_{avg}^P can be compared with the minimum number of time-steps necessary to finish production works, T_{min}^P. This can only happen in an ideal case where all robots work for production without any random walking or failure. We can get T_{min}^P from the total amount of work load and maximum possible inputs from all robots. If there are N robots, each machine has Φ_{INIT}^P task-urgency, and each time-step robots can decrease N $\times$ $\Delta\phi_{DEC}$ task-urgencies, then the theoretical T_{min}^P can be found from the following Eq. 5.

$$T_{min}^P = \frac{J \times \Phi_{INIT}^P}{N \times \Delta\phi_{DEC}} \tag{5}$$

$$\zeta_{avg}^P = \frac{T_{avg}^P - T_{min}^P}{T_{min}^P} \tag{6}$$

Thus we can define ζ_{avg}^P, average production completion delay (APCD) by following Eq. 6: After a machine enters into maintenance cycle, if no robot serves a machine, the growth of task-urgency will follow Eq. 2. However, if ν_k robots are serving this

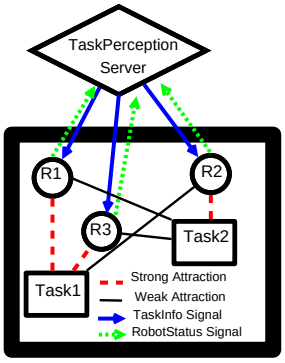

Fig. 3: A centralized communication scheme

machine at a particular time-step k^{th} , task-urgency at $(k+1)^{th}$ time-step can be represented by:

$$\Phi^M_{j,k+1} = \Phi^M_{j,k} - (\nu_k - \mu) \times \Delta\phi_{DEC} \quad (7)$$

By considering $\mu = 1$, Eq. 7 will reduces to Eq. 3. Here, $\Phi^M_{j,k+1}$ will correspond to the *pending maintenance work-load* of a particular machine at a given time. This happens due to the random task switching of robots with random-walking options. We can find the *average pending maintenance work-load* (APMW) per time-step in each machine, χ^M_j (Eq. 8) and average PMW per machine per time-step, χ^M_{avg} (Eq. 9).

$$\chi^M_j = \frac{1}{K}\sum_{k=1}^{K} \Phi^M_{j,k} \quad (8) \qquad \chi^M_{avg} = \frac{1}{J}\sum_{j=1}^{M} \chi^M_j \quad (9)$$

V. Communication Models

A. Centralized communication model

AFM relies upon a system-wide continuous flow of information which can be realized using any suitable communication model. A simple centralized communication scheme is outlined in Fig. 3. In this model we have used bi-directional signal-based exchange of communication messages between a centralized *task perception server* (TPS) and a *robot-controller client* (RCC) e.g. R1, R2 etc. The main role of TPS is to send up-to-date task-information to RCCs for running their task-allocation algorithms. The urgency value of each task is dynamically updated by TPS after receiving the status signals from the working robots of that particular task. Fig. 3 shows how three robots are attracted to two different tasks and their communications with TPS. This communication helps the robots to gain information that can be treated as "global sensing". However in this model robots do not communicate among themselves. Hence this model can be approximated as the GSNC strategy.

B. Local communication model

In most swarm robotic research local communication is considered as the one of the most critical components of the swarms where the global behaviours emerges from the local interactions among the individuals and their environment. In this study, we have used the concepts of pheromone active-space of ants to realize LSLC. Ants use various chemical pheromones with different active spaces (or communication ranges) to communicate different messages with their group members [23]. Ants sitting near the source of this pheromone sense and respond quicker than others who wander in far distances. Thus both communication and sensing occurs within a small communication range[1]. We have used this concept of communication range or locality in our local communication model. A suitable range (or radius) of communication and sensing can be set at design time based on the capabilities of robots [15]. Alternately they can also be varied dynamically over time depending on the cost of communication and sensing, e.g. density of peers, ambient noise in the communication channels, or even by aiming for maximizing information spread [24]. In this study, we have followed the former approach as our robots do not have the precise hardware to dynamically vary their communication and sensing ranges.

In our local communication model we have assumed that robots can communicate to its nearby peers within a certain communication radius, r_{comm} and they can sense tasks within another radius r_{task}. A robot R_1 is a *peer* of robot R_2, if spatial

[1]Here, we have broadly viewed sensing as the part of communication process, either implicitly via environment, or explicitly via local peers.

distance between R_1 and R_2 is less than this r_{comm}. Similarly, when a robot comes within this r_{task} of a task, it can sense the status of this task.

We can characterize our local communication model in terms of message content, communication frequency and target recipients [25]. Robots can communicate with their peers with any kind of message. Robots communicate only when they meet their peers within r_{comm}. In terms of target recipients, our model differs from a traditional publish/subscribe communication model by introducing the concept of dynamic subscription. In a traditional publish/subscribe communication model, subscription of messages happens prior to the actual message transmission. In that case prior knowledge about the subjects of a system is necessary. But in our model this is not necessary as long as all robots uses a common addressing convention for naming their incoming signal channels. In this way, when a robot meets with another robot it can infer the address of this peer robot's channel name by using a shared rule. A robot is thus always listening to its own channel for receiving messages from its potential peers or message publishers. On the other side, upon recognizing a peer, a robot sends a message to this particular peer. So here neither it is necessary to create any custom subject namespace [25] nor we need to hard-code information in each robot controller about the knowledge of their potential peers *a priori*.

VI. Experimental design

The overall aim of our MRTA experiments is to compare the various properties of self-regulated MRTA under both GSNC and LSLC strategies. These experiments are grouped into four series labelled using the following letters: *A, B, C* and *D*. Series A and B experiments are done using a centralized communication system under GSNC strategy and Series C and D experiments are carried out using an emulated local P2P communication under LSLC stategty.

Self-regulated MRTA is often characterised by plasticity and task-specialization [26]. Within our manufacturing shop-floor context, *plasticity* refers to the collective ability of the robots to switch from random-walking to doing a task (or vice-versa) depending on the work-load present in the system. Here we expect to see that most of the robots would be able to engage in tasks when there would be high workloads (or task-urgencies). The changes of task-urgencies and the ratio of robots engaged in tasks can be good metrics to observe plasticity in MRTA. Self-regulated MRTA is generally accompanied with *task-specializations* of agents. That means that few robots will be more active than others. From the interpretation of AFM, we can see that after doing a task a few times, a robot will soon be sensitized to it. Therefore, from the raw log of task sensitization of robots, we can be able to trace the pattern of task-sensitization of robots per task basis.

We can measure the quality of MRTA from the shop-floor production completion time i.e. APCD that indicates how much more time is spent in the production process due to the self-organization of robots. In order to calculate APCD, we can find the production completion time for each task from the raw log of task-urgency. In order to see if our system can respond to the gradually increasing workloads, we can measure shop-floor maintenance delay i.e. APMW that can show the robustness of our system. When a task is not being served by any robot for some time we can see that its urgency will rise and robots will respond to this dynamic demand. For measuring APMW we need only the task-urgency data.

In order to characterize the energy-efficiency in MRTA we can log the pose data of each robot that can give us the total translations occurred by all robots in our experiments. This can give us a rough indication of energy-usage by our robots. Since AFM requires a system-wide continuous flow of information, we can measure the communication load to bench-mark our implementation of communication system. Here we can measure how much task-related information is sent to the robots at each time step.

In order to see the effects of scaling on MRTA, we have designed two group of experiments. Series A corresponds to a small group where we have used 8 robots, 2 tasks under an arena of 2 m^2. We have

TABLE I: Experimental parameters of Series A & B

Parameter	Value
Initial production work (Ω_j^p) unit	100
Task urgency increase rate ($\Delta\phi_{INC}$)	0.005
Task urgency decrease rate ($\Delta\phi_{DEC}$)	0.0025
Initial sensitization (K_{INIT})	0.1
Sensitization increase rate (Δk_{INC})	0.03
Sensitization decrease rate (Δk_{DEC})	0.01

doubled these numbers in Series B, C and D, i.e. 16 robots, 4 tasks under an arena of 4 m^2. This proportional design can give us a valuable insight about the effects of scaling on self-regulated MRTA. Table I lists a set of essential parameters of our experiments. The initial values of task urgencies correspond to 100 units of production work-load without any maintenance work-load as outlined in Eq. 1. We choose a limit of 0 and 1, where 0 means no urgency and 1 means maximum urgency. Same rule applies to sensitisation. This also implies

Fig. 4: Our multi-robot experiment arena

that if sensitization is 0, task has been forgotten completely and if sensitization is 1, the task has been learnt completely.

In Series C and D, both communication and sensing range values are kept same. Series D uses 1m ranges that enables our robot to capture more task information at a time. That is similar to "global sensing" of information by the robots. Series C uses the half of the range values of Series D (0.5m). This enables our robots to capture less information, that closely mimics a LSLC strategy.

VII. Implementation

Ideally, AFM can be implemented as a complete distributed task-allocation system where each agent selects its own task based on its own external perception about task-urgencies (i.e. attractive fields), distances from tasks and internal task-sensitisation records. Such an implementation requires powerful robots with sophisticated sensors (camera, laser etc.) and sufficient computation and communication capabilities. However, in this study, we are particularly interested to find the suitable communication schemes that can effectively spread the attractive fields (task-urgencies) among robots. So we have simplified the complexities of a full-fledged implementation by using a centralized communication system that effectively makes up the limitations of our e-puck[2] robots.

In our current implementation we emulate a manufacturing shop-floor scenario that requires the robot only to travel among tasks. These robots are controlled autonomously from a host PC by using BTCom Bluetooth communication protocol over the wireless link. Thus our host-PC runs one RCC for each physical robot. As shown in Fig. 4 robots move to the target tasks represented by rectangular boxes. The detail implementation of software components of our multi-robot control architecture has been discussed in [22].

VIII. Results

In this section we have presented our experimental results. We ran those experiments for about 40 minutes duration. They are averaged over five iterations for Series A and B experiments and three iterations for Series C and D experiments.

A. Shop-floor work-load history

In our experiments we have defined shop-floor work-load in terms of task urgencies. Fig. 5 shows the dynamic changes in task-urgencies for the single iteration of one of the Series D experiments. The fluctuations in this plot is resulted from the different levels of task-performance of our robots. Here, we can see that an unattended task, *Task4*, was

[2]www.e-puck.org

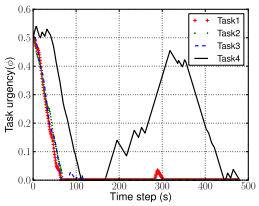

Fig. 5: Changes in task-urgencies.

not served by any robot for a long period and later it was picked up by some of the robots. In order to measure the task-related work-loads on our system we have summed up the changes in all task-urgencies over time. We call this as *shop-floor work-load history* and formalized as follows. Let $\phi_{j,q}$ be the urgency of a task j at q^{th} step and $\phi_{j,q+1}$ be the task urgency of $(q+1)^{th}$ step. We can calculate the sum of changes in urgencies of all J tasks at $(q+1)^{th}$ step:

$$\Delta\Phi_{j,q+1} = \sum_{j=1}^{J}(\phi_{j,q+1} - \phi_{j,q}) \qquad (10)$$

Fig. 6 shows the dynamic shop-floor workload for all four series of experiments.

B. Ratio of active workers

From Fig. 7, we can see that in production cycle, when work-load is high, many robots are active in tasks. Here active workers ratio is the ratio of those robots that work on tasks to the total number of robots (N) of a particular experiment. This ratio varies according to the shop-floor work-load changes.

C. Shop-task performance

As shown in Table II both Series C and Series D experiments show similar production delay (APCD) values: 605s and 615s respectively, which are less than Series B experiment result (825s) and are close to Series A experiment result (555s). Note that all statistical t-test results are obtained with respect to Series C data and it shows that there is no significant difference in task-performance between Series B and Series C results.

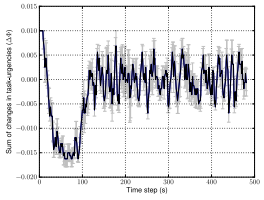

(a) Series A

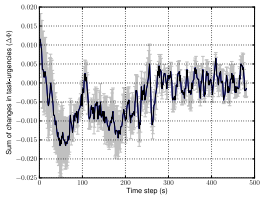

(b) Series B

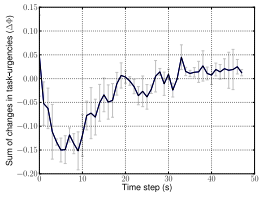

(c) Series C

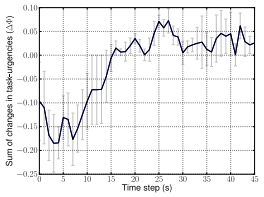

(d) Series D

Fig. 6: Shop-floor workload history starting clockwise from top left for Series A-D.

D. Task specializations

We have measured the task-specialization of the robots based-on their peak sensitization values. This maximum value represents how long a robot has repeatedly been selecting a particular task. Since tasks are homogeneous we have considered the maximum sensitization value of a robot among all tasks during an experiment run. This value is then

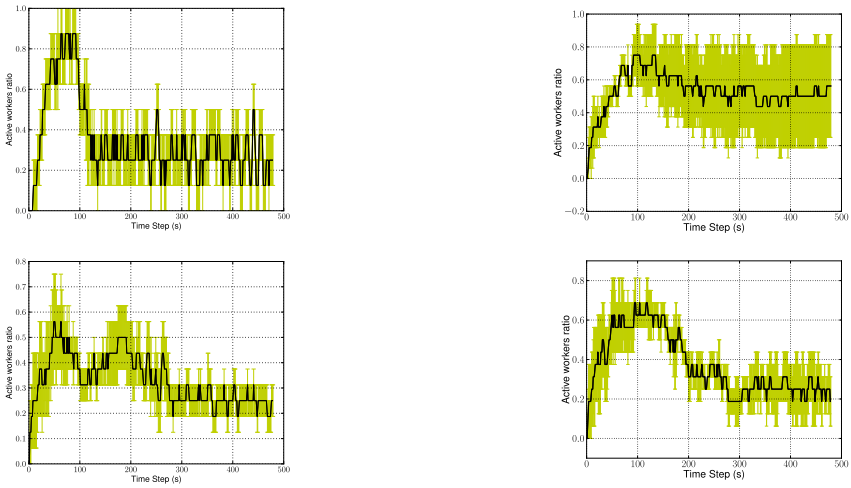

Fig. 7: Self-organized allocation of robots starting clockwise from top left Series A-D.

TABLE II: Shop-floor task performance

Series	APCD (SD) s	*p-value* 1-tailed t-test (confidence)	APMW (SD) s	*p-value* 1-tailed t-test
A	555 (50)	0.0	5 (5)	0.0
B	825 (360)	0.2 (60%)	15 (65)	0.0
C	605 (180)	N/A	25 (85)	N/A
D	615 (200)	0.0	10 (35)	0.0

TABLE III: Task-specialization of the robots

Series	K^G_{avg} (SD)	*p-value* 1-tailed t-test (confidence)	Q^G_{avg} (SD)	*p-value* 1-tailed t-test (confidence)
A	0.40 (0.08)	0.0	38 (13)	0.001 (99.8%)
B	0.30 (0.03)	0.2 (60%)	18 (5)	0.2 (60%)
C	0.39 (0.17)	N/A	13 (7)	N/A
D	0.27 (0.1)	0.0	11 (5)	0.0

averaged for all robots using the following equation.

$$K^G_{avg} = \frac{1}{N}\sum_{i=1}^{N} \max_{j=1}^{M} \left(k^i_{j,q}\right) \tag{11}$$

If a robot r_i has the peak sensitization value k^i_j on task j ($j \in M$) at q^{th} time-step, Eq. 11 calculates the average of the peak task-specialization values of all robots for a certain iteration of our experiments. We have also averaged the time-step values (q) taken to reach those peak values for all robots using the following equation.

$$Q^G_{avg} = \frac{1}{N}\sum_{i=1}^{N} q^i_{k=k_{max}} \tag{12}$$

In Eq. 12, $q^i_{k=k_{max}}$ represents the time-step of robot r_i where its sensitization value k reaches the peak k_{max} as discussed above. By averaging this peak time-step values of all robots we can have an overall idea of how many task-execution cycles are spent to reach the maximum task-specialization value K^G_{avg}.

As shown in Table III, the overall task-specialization of group in Series C is closer to that of Series A experiments and interestingly, the value of Series D is much closer to that of Series B experiments. So task-specialization in large group under LSLC strategy is not significantly different than their GSNC counter part.

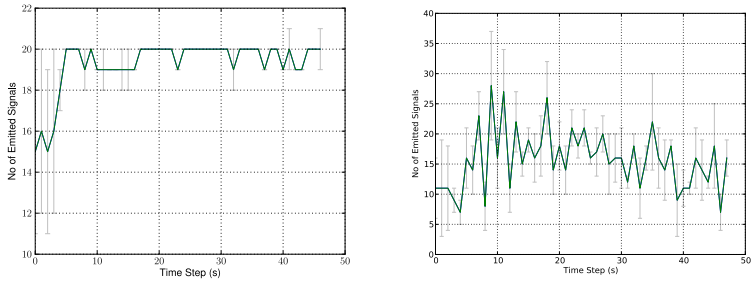

(a) Series A (b) Series C

Fig. 8: Frequency of `TaskInfo` signalling of (a) by TPS and (b) by local peers.

E. Communication load

Fig. 8 (a) shows the number of received `TaskInfo` signals by each robot in Series A experiments. The duration of each time-step is 50s long and TPS emits signal in every 2.5s in both Series A and B experiments. The overall P2P task information signals of both of these local modes varied according to the dynamic number of local peers are plotted in Fig. 8 (b).

F. Robot motions

TABLE IV: Sum of translations of robots.

Series	Average translation (SD) m	*p-value* 1-tailed t-test (confidence)
A	2.631 (0.804)	N/A
B	13.882 (3.099)	0.001 (99.8%)
C	4.907 (1.678)	N/A
D	4.854 (1.592)	0.0

We have aggregated the changes in translation motion of all robots over time based on their travelled distances in Euclidean metric. Let $u_{i,q}$ and $u_{i,q+1}$ be the translations of a robot i in two consecutive steps. If the difference between these two translations be δu_i, we can find the sum of changes of translations of all robots in $(q+1)^{th}$ step using the following equation.

$$\Delta U_{q+1} = \sum_{i=1}^{N} \delta u_{i,q+1} \tag{13}$$

Table IV summarizes the average translations done by robots in all four series of experiments. Here we have found that under LSLC strategy, robot translations have been reduced significantly, i.e. Series C and Series D show about 2.8 times less translation than that of in Series B experiments. The translation of 16 robots in Series C and Series D experiments are approximately double (1.89 times) than that of Series A experiments with 8 robots.

IX. Discussions

From our comparative results, we note that for large group of robots, degradation in task-performance and task-specialization of robots are likely to occur under GSNC strategy that relies upon a centralized communication system. This confirms us the assertions made by some biologists that self-regulated DOL among small group of individuals can happen without any significant amount of local communications and interactions [26]. However, our findings suggest that task-specialization can still be beneficial among the individuals of a small group which contradicts the claim that small groups only posses the generalist workers, but not the specialists. On the other hand, LSLC strategy is more suitable for large group of individuals that are likely to be unable to perform global sensing and global communication with all individuals of the group. The design of communication and sensing range still remains as a critical research issue. However, our results suggest that the idea of maximizing information gain is not appropriate under a stochastic task-allocation process. Here more information tends to cause more task-switching behaviours that lowers the level of task-specialization of the group.

X. Conclusion and future work

This study focuses on comparing two bio-inspired communication and sensing strategies in producing self-regulated MRTA by AFM. Under both centralized and local communication strategies, AFM has produced the desired self-regulated MRTA among a group of 8 and 16 robots. Despite having the limited communication and sensing range, local strategy has helped the robots to produce comparatively better task-allocation with increased task-specialization and significantly reduced motions or savings in energy consumption.

This study can possibly be extended in co-operative task domains where different individuals with a variety of task-skills interact with each other directly. AFM can be applied to a more challenging real-world environment with suddenly appearing (and disappearing) tasks. Moreover, experiments can be carried out using non-random robot distributions to find out any performance variation.

References

[1] L. E. Parker and F. Tang, "Building multirobot coalitions through automated task solution synthesis," *Proceedings of the IEEE*, vol. 94, pp. 1289–1305, 2006.

[2] B. P. Gerkey and M. J. Mataric, "A formal analysis and taxonomy of task allocation in multi-robot systems," *International J. of Robotics Research*, vol. 23, p. 939, 2004.

[3] A. B. Sendova-Franks and N. R. Franks, "Self-assembly, self-organization and division of labour'," *Philosophical Transactions of the Royal Society of London B*, vol. 354, pp. 1395–1405, 1999.

[4] B. Gerkey and M. Mataric, "Multi-robot task allocation: analyzing the complexity and optimality of key architectures," *Robotics and Automation, 2003. Proceedings. ICRA'03. IEEE International Conference on*, vol. 3, 2003.

[5] E. Arcaute, K. Christensen, A. Sendova-Franks, T. Dahl, A. Espinosa, and H. J. Jensen, "Division of labour in ant colonies in terms of attractive fields," *Ecol. Complexity*, 2008.

[6] R. Jeanne, "Group size, productivity, and information flow in social wasps," *Information processing in social insects*, pp. 3–30, 1999.

[7] L. E. Parker, "Alliance: an architecture for fault tolerant multirobot cooperation," *Robotics and Automation, IEEE Transactions on*, vol. 14, pp. 220–240, 1998.

[8] L. Chaimowicz, M. F. M. Campos, and V. Kumar, "Dynamic role assignment for cooperative robots," *Robotics and Automation, 2002. Proceedings. ICRA'02. IEEE International Conference on*, vol. 1, 2002.

[9] R. Zlot, A. Stentz, M. Dias, and S. Thayer, "Multi-robot exploration controlled by a market economy," *Robotics and Automation, 2002. Proceedings. ICRA'02. IEEE International Conference on*, vol. 3, 2002.

[10] K. Lerman, C. Jones, A. Galstyan, and M. J. Mataric, "Analysis of dynamic task allocation in multi-robot systems," *The International Journal of Robotics Research*, vol. 25, p. 225, 2006.

[11] S. Camazine, N. Franks, J. Sneyd, E. Bonabeau, J. Deneubourg, and G. Theraula, *Self-organization in biological systems*. Princeton, N.J. : Princeton University Press, 2001.

[12] E. Bonabeau, M. Dorigo, and G. Theraulaz, *Swarm intelligence: from natural to artificial systems*. Oxford University Press, 1999.

[13] W. Liu, A. F. T. Winfield, J. Sa, J. Chen, and L. Dou, "Towards energy optimization: Emergent task allocation in a swarm of foraging robots," *Adaptive Behavior*, vol. 15, no. 3, pp. 289–305, 2007.

[14] M. Krieger and J. Billeter, "The call of duty: Self-organised task allocation in a population of up to twelve mobile robots," *Robotics and Autonomous Systems*, vol. 30, no. 1-2, pp. 65–84, 2000.

[15] W. Agassounon and A. Martinoli, "Efficiency and robustness of threshold-based distributed allocation algorithms in multi-agent systems," in *Proc. of the first international joint conference on Autonomous agents and multiagent systems: part 3*, 2002.

[16] C. Jones and M. Mataric, "Adaptive division of labor in large-scale minimalist multi-robot systems," in *Proc. of IEEE/RSJ Int'l Conference on Intelligent Robots and Systems, 2003 (IROS 2003)*, 2003.

[17] N. Kalra and A. Martinoli, "A comparative study of market-based and threshold-based task allocation," *Distributed Autonomous Robotic Systems 7*, pp. 91–101, 2007.

[18] B. B. Werger and M. J. Mataric, "Broadcast of local eligibility for multi-target observation," *Distributed Autonomous Robotic Systems*, vol. 4, p. 347356, 2001.

[19] S. Botelho, R. Alami, and T. LAAS-CNRS, "M+: a scheme for multi-robot cooperation through negotiated taskallocation and achievement," *Proceedings IEEE International Conference on Robotics and Automation*, vol. 2, 1999.

[20] B. P. Gerkey and M. J. Mataric, "Sold!: Auction methods for multirobot coordination," *IEEE Transaction on Robotics and Automation*, vol. 18, 2002.

[21] H. Çelikkanat, A. Turgut, and E. Şahin, "Guiding a robot flock via informed robots," *Distributed Autonomous Robotic Systems 8*, pp. 215–225, 2008.

[22] M. O. F. Sarker, "Self-regulated multi-robot task allocation," Ph.D. dissertation, University of Wales, Newport, 2010.

[23] B. Holldobler and E. Wilson, *The ants*. Belknap Press, 1990.

[24] E. Yoshida and T. Arai, "Performance analysis of local communication by cooperating mobile robots," *IEICE Transactions on Communications*, vol. 83, no. 5, 2000.

[25] B. Gerkey and M. Mataric, "Principled communication for dynamic multi-robot task allocation," *Experimental Robotics VII*, pp. 353–362, 2001.

[26] S. Garnier, J. Gautrais, and G. Theraulaz, "The biological principles of swarm intelligence," *Swarm Intelligence*, vol. 1, no. 1, pp. 3–31, 2007.